

수평 곡선보의 자유진동 해석 Free Vibrations of Horizontally Curved Beams

이 병 구* 오 상 진**
Lee, Byoung Koo Oh, Sang Jin

ABSTRACT

The differential equations governing free, out of plane vibrations of horizontally curved beams are derived and solved numerically to obtain the natural frequencies and the mode shapes. The Runge-Kutta method and Regula-Falsi method are used to integrate the differential equations and to determine the natural frequencies, respectively. In numerical examples, the hinged-clamped end constraint is considered and four lowest frequency parameters are reported as functions of four non-dimensional system parameters: (1) opening angle, (2) slenderness ratio, (3) shear parameter and (4) stiffness parameter. Also, typical mode shapes of displacements and stress resultants are shown.

1. INTRODUCTION

Since horizontally curved beams are basic structural forms, their dynamics and especially free vibrations have been studied extensively. References^[1-5] and their citations include the governing equations and the significant historical literature on the out of plane free vibrations of uniform, linearly elastic curved beams of various geometries and end constraints. Briefly, the exact solutions of natural frequencies have been studied by Archer^[1], Morely^[2] and Ojalvo^[3]. Approximate methods have been developed in calculating the natural frequencies of curved beams. Such works included studies by Den Hartog^[4], Voltera and Morell^[5].

To the knowledge of the authors, no investigation has been made into the free vibrations of horizontally curved beams using the numerical method in which the numerical integration scheme and the bracketing method are combined with. The main purpose of this paper is, therefore, to present such a numerical method for calculating the natural frequencies of horizontally curved beams.

2. GOVERNING EQUATIONS

The geometry of uniform circular horizontally curved beam is defined in Figure 1. The two ends are supported by the hinged or clamped end constraint. Its opening angle and radius of curved beam are α and a , respectively. The radius of arbitrary point of beam has an inclination θ with that of left end. Also shown in Figure 1 are the positive direction of vertical displacement v , positive directions of rotations ψ and β

* Professor, Wonkwang University

** Graduate Student, Wonkwang University

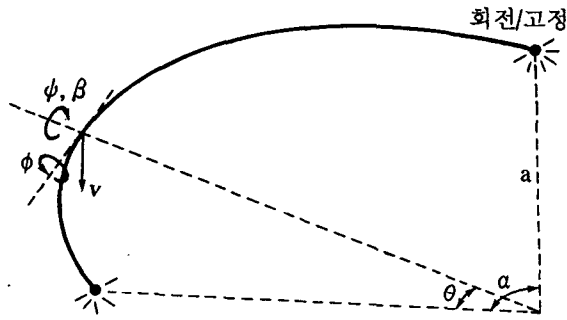


Fig. 1 Curved beam and displacements

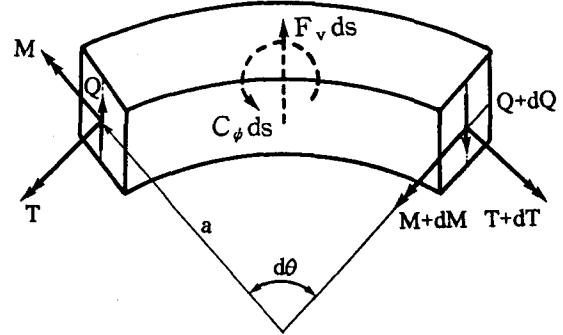


Fig. 2 Loads on a curved beam element

of cross-section due to the bending moment and shear force, respectively, and positive direction of angle of twist ϕ .

A small element of the curved beam with the opening angle $d\theta$ and arc length ds shown in Figure 2 defines the positive directions for the shear forces Q , the bending moments M , the torsional moments T , the vertical inertia force F_v and the rotatory inertia couple C_ϕ . With the inertia force and the rotatory inertia couple treated as equivalent static quantities, the three equations for dynamic equilibrium of element are:

$$\frac{dQ}{d\theta} - aF_v = 0, \quad \frac{dM}{d\theta} - aQ + T + aC_\phi = 0, \quad M - \frac{dT}{d\theta} = 0 \quad (1 \sim 3)$$

The equations that relate M and T to the rotations ψ and ϕ are as follows.

$$M = \frac{EI}{a} \left(\phi - \frac{d\psi}{d\theta} \right), \quad T = \frac{JG}{a} \left(\psi + \frac{d\phi}{d\theta} \right) \quad (4,5)$$

where E =Young's modulus, G =shearing modulus, I =area moment of inertia and J =polar moment of inertia of cross-section.

The total angle between the deformed and undeformed cross-section of the beam is:

$$\frac{dv}{ds} = \frac{1}{a} \frac{dv}{d\theta} = \psi + \beta \quad (6)$$

in which β is the angle of shear. The transverse shear force Q is given by^[6]

$$Q = k\beta AG = kAG \left(\frac{1}{a} \frac{dv}{d\theta} - \psi \right) \quad (7)$$

in which A is the cross-sectional area, and k is the cross-sectional shape factor. For examples, the k value for a rectangular and a circular section are $5/6$ and $3/4$, respectively. In an I beam k is approximately equal to A_w/A , where A_w is the area of web. For rolled sections, A_w/A ranges from about 0.2 to 0.5.

The curved beam is assumed to be in harmonic motion, or each co-ordinate is proportional to $\sin \omega t$, where ω is the angular frequency and t is time. The inertia loadings are then

$$F_v = -m\omega^2 v, \quad C_\phi = -m\omega^2 r^2 \psi \quad (8,9)$$

where m =mass per unit length and r =radius of gyration of cross-section.

When equations (4), (5) and (7) are differentiated once, the results are

$$\frac{dM}{d\theta} = \frac{EI}{a} \left(\frac{d\phi}{d\theta} - \frac{d^2\phi}{d\theta^2} \right), \quad \frac{dT}{d\theta} = \frac{IG}{a} \left(\frac{d\phi}{d\theta} + \frac{d^2\phi}{d\theta^2} \right), \quad \frac{dQ}{d\theta} = kAG \left(\frac{1}{a} \frac{d^2v}{d\theta^2} - \frac{d\phi}{d\theta} \right) \quad (10 \sim 12)$$

To facilitate the numerical studies, the following non-dimensional system parameters are defined as follows:

$$\eta = v/a, \quad \lambda = a/r, \quad \gamma = kG/E, \quad \varepsilon = JG/EI \quad (13 \sim 16)$$

where η = non-dimensional vertical displacement, λ = slenderness ratio, γ = shear parameter and ε = stiffness parameter.

When equations (8) and (12) are substituted into equation (1) and the non-dimensional forms of equations (13)~(16) are used, the result is

$$\frac{d^2\eta}{d\theta^2} = -\frac{p_i^2}{\gamma\lambda^2} \eta + \frac{d\phi}{d\theta} \quad (17)$$

When equations (5), (7), (9) and (10) are substituted into equation (2) and the non-dimensional forms of equations (13)~(16) are used, the result is

$$\frac{d^2\phi}{d\theta^2} = -\gamma\lambda^2 \frac{d\eta}{d\theta} + \left(\gamma\lambda^2 + \varepsilon - \frac{p_i^2}{\lambda^2} \right) \phi + (1 + \varepsilon) \frac{d\phi}{d\theta} \quad (18)$$

When equations (4) and (11) are substituted into equation (3) and the non-dimensional forms of equations (13)~(16) are used, the result is

$$\frac{d^2\phi}{d\theta^2} = -\left(1 + \frac{1}{\varepsilon} \right) \frac{d\phi}{d\theta} + \frac{1}{\varepsilon} \phi \quad (19)$$

In equations (17) and (18), the p_i is the non-dimensional frequency parameter defined as

$$p_i = \omega_i a^2 (m/EI)^{1/2} \quad (20)$$

which is written in terms of the i th frequency $\omega = \omega_i$, $i=1,2,3,4,\dots$.

For the hinged end at $\theta=0$ or $\theta=\alpha$, the boundary conditions are

$$\eta = 0, \quad \phi' = 0, \quad \phi = 0 \quad (21 \sim 23)$$

For the clamped end at $\theta=0$ or $\theta=\alpha$, the boundary conditions are

$$\eta = 0, \quad \phi = 0, \quad \phi = 0 \quad (24 \sim 26)$$

Beam stresses may be computed from the following non-dimensional forms for the bending moment M , the torsional moment T and shear force Q . The respective results obtained from equations (4), (5) and (7) using equation (13) are:

$$\bar{M} = \frac{Ma}{EI} = \phi - \frac{d\phi}{d\theta}, \quad \bar{T} = \frac{Ta}{JG} = \phi + \frac{d\phi}{d\theta}, \quad \bar{Q} = \frac{Q}{kAG} = \frac{d\eta}{d\theta} - \phi \quad (27 \sim 29)$$

3. NUMERICAL METHOD AND VALIDATION

Based on the above analysis, a general FORTRAN computer program was written to calculate p_i , $\eta = \eta_i(\theta)$, $\phi = \phi_i(\theta)$, $\phi = \phi_i(\theta)$, $\bar{M} = \bar{M}_i(\theta)$, $\bar{T} = \bar{T}_i(\theta)$, $\bar{Q} = \bar{Q}_i(\theta)$. First, the Regula-Falsi method was used to calculate the characteristic values p_i ; and then the Runge-Kutta method was used to calculate the mode shapes. In the free vibration of horizontally curved beam, such a numerical method was developed for the first time

in this paper. The numerical procedure developed herein is summarized as follows.

- (1) Specify the curved beam geometry (support constraint, α , λ , γ , ε), and set of three homogeneous boundary constraints which are either equations (21)~(23) or (24)~(26).
- (2) Consider sixth order system, equations (17)~(19), as three initial value problems whose initial values are the three homogeneous boundary constraints $\theta=0$, as chosen in step 1. Then assume a trial frequency parameter p_i in which the first trial value is zero.
- (3) With the numerical integration technique in which the Runge-Kutta method^[7] was used, integrate equations (17)~(19) from $\theta=0$ to $\theta=\alpha$. Perform three separate integrations, one for each of the three boundary constraints.
- (4) From the Runge-Kutta solution, evaluate at $\theta=\alpha$ the determinant D of the coefficient matrix for the boundary conditions of equations (21)~(30) or (24)~(26). If $D=0$, then the trial value of p_i is an eigenvalue. If $D \neq 0$, then increment p_i and repeat the above calculations.
- (5) Repeat steps 3 and 4 and note the sign of D in each iteration. If D changes between two consecutive trials, then the eigenvalue lies between these last two trial values of p_i .
- (6) Use the Regula-Falsi method^[8], one of the bracketing methods, to compute the advanced trial p_i based on its two previous values.
- (7) Terminate the calculations and print the value of p_i and corresponding mode shapes when the convergence criteria are met.

In numerical examples, the hinged-clamped beams were considered and the lowest four frequencies were calculated. For these studies, suitable convergence of solutions was obtained for an increment of $\Delta=\alpha/50$ referred on the Figure 4 in which the convergence analysis is shown. The convergence criterion was that p_i solutions obtained with the $\alpha/50$ increment agreed with those obtained with the $\alpha/100$ increment to within three significant figures.

For comparison purposes, the finite element solutions based on the commercial package SAP90 were used to compute the first four frequency parameters p_i . The results are shown in Table 1 in which the frequencies of this study agree closely with those of SAP90 within a tolerance of 2%. These comparisons serve to validate the numerical method developed herein conclusively.

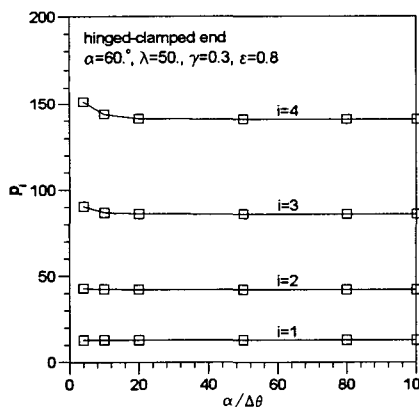


Fig. 3 Convergency analysis

Table 1. Comparison of frequency parameter p_i between this study and SAP90

Geometry of curved beam	i	Frequency parameter, p_i		Error(%)	
		This study(A)	SAP90(B)		(A-B)/A
hinged-clamped $\lambda=770$ $\gamma=0.32$ $\varepsilon=1.54$	$\alpha=30^\circ$	1	55.25	55.66	-0.74
		2	181.0	182.4	-0.77
		3	378.5	379.9	-0.37
		4	647.4	649.0	-0.25
	$\alpha=60^\circ$	1	13.13	13.26	-0.99
		2	44.43	44.67	-0.54
		3	93.84	95.33	-1.59
		4	161.3	162.8	-0.93

4. COMPUTED RESULTS AND DISCUSSION

It is shown in Figure 4 for which hinged-clamped beam, $\lambda=50$, $\gamma=0.3$ and $\varepsilon=0.8$, that the frequency parameters p_i decrease as the opening angle α is increased generally. It is observed that p_i values all decrease very rapidly α increases from about 30 deg to 100 deg. Further, the p_i approach lower limits or horizontal asymptotes as α increase.

In Figure 5, hinged-clamped beam, $\alpha=90$ deg, $\gamma=0.3$, $\varepsilon=0.8$ and p_i increases as λ increases. The increasing slope is very steep when λ is less than 50. And it is clear that the effect of λ is greater in the higher mode than in lower mode in this range of λ , i. e. less than about 50. Also, the p_i values approach upper limits or horizontal asymptotes as λ increases to 200.

Figure 6 shows the relationship between p_i and γ for hinged-clamped beam with $\alpha=60$ deg, $\lambda=50$ and $\varepsilon=0.8$. It is seen that the effect of γ on p_i is similar to the Figure 5 represented p_i vs. λ .

Shown in Figure 7, hinged-clamped beam, $\alpha=60$ deg, $\lambda=50$ and $\gamma=0.3$, are the p_i versus ε curves. The p_i increases as the ε increases. But the increasing rate of p_i is very small in the range of $\varepsilon > 0.1$.

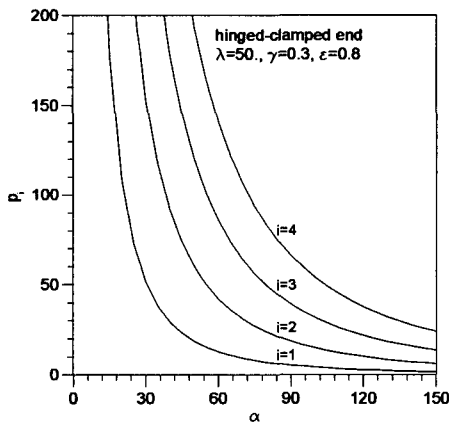


Fig. 4 p_i vs. α curves

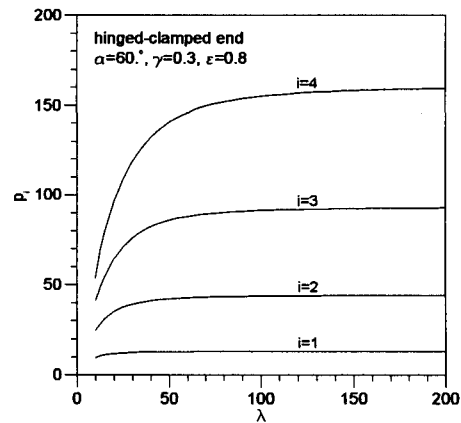


Fig. 5 p_i vs. λ curves

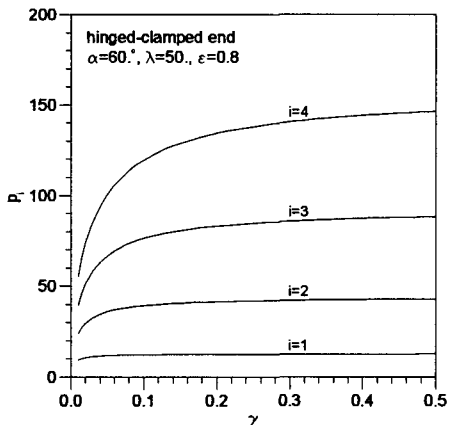


Fig. 6 p_i vs. γ curves

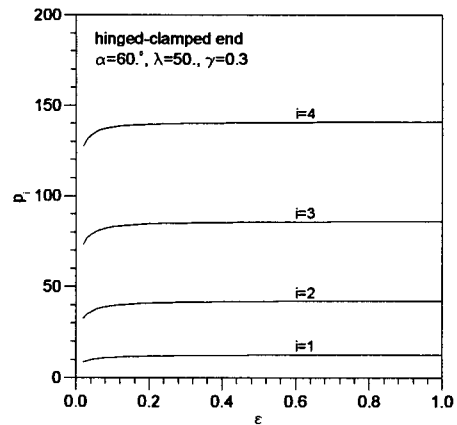


Fig. 7 p_i vs. ε curves

Typical second mode shapes of displacements and stress resultants are shown in Figures 8 and 9, respectively, based on the hinged-clamped end, $\alpha=60$ deg, $\lambda=50$ and $\gamma=0.3$ and $\varepsilon=0.8$.

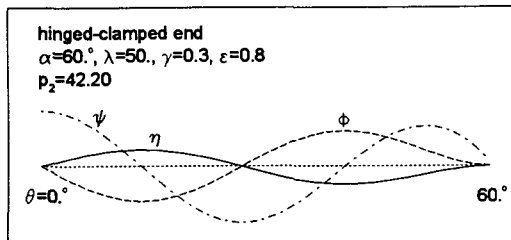


Fig. 8 Example of second mode shapes of displacements

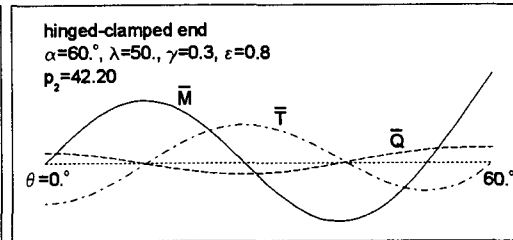


Fig. 7 Example of second mode shapes of stress resultants

5. CONCLUSIONS

The method presented here for calculating frequencies for horizontally curved beam was found to be efficient, robust and reliable over a wide range of system parameters.

Computations showed that the frequency parameters p_i increase as the slenderness ratio λ , shear parameter γ and stiffness parameter ε increase, other non-dimensional system parameters remaining same, while the p_i decreases as the opening angle α increases.

ACKNOWLEDGEMENT

This paper was supported by NON-DIRECTED RESEARCH FUND, Korea Research Foundation in 1994. The authors thank for the financial support.

REFERENCES

1. R.R. Archer: Small Vibrations of Thin Incomplete Circular Rings, International Journal of Mechanical Sci., Vol. 1, 1960, pp.45-46.
2. L.S.D Morley: The Flexural Vibrations of a Cut Thin Ring, Quarterly Journal of Mechanics and Applied Math., Vol. 11, 1934, pp.429-449.
3. T.V. Ojalvo: Coupled Twist-Bending Vibrations of Incomplete Elastic Rings, International Journal of Mechanical Science, Vol. 4, 1972, pp.53-72.
4. J.P. Den Hartog: The Lowest Natural Frequency of Circular Arc, Philosophical Magazine, Series 7, Vol. 5, 1928, pp.400-408.
5. E. Volterra and J.D. Morell: A note on the Lowest Natural Frequency of Elastic Arcs, Journal of the Applied Mechanics, Vol. 27, 1960, pp.744-746.
6. J.M. Gere and S.P. Timoshenk: Mechanics of Materials, Brooks Cole Engineering Division, 1984.
7. B. Carnahan, H.A. Luther and Wilkes, J.O.: Applied Numerical Methods, John Wiley & Sons, 1969.
8. J.H. Ferziger: Numerical Method for Engineering Application, John Wiley & Sons, 1981.